

Document downloaded from:

<http://hdl.handle.net/10251/49064>

This paper must be cited as:

Escrivá Cerdán, C.; Blasco Tamarit, ME.; García García, DM.; García Antón, J.; Guenbour, A.; Guenbour, A. (2012). Passivation behaviour of Alloy 31 (UNS N08031) in polluted phosphoric acid at different temperatures. *Corrosion Science*. 56:114-122.
doi:10.1016/j.corsci.2011.11.014.



The final publication is available at

<http://dx.doi.org/10.1016/j.corsci.2011.11.014>

Copyright Elsevier

PASSIVATION BEHAVIOUR OF ALLOY 31 IN POLLUTED PHOSPHORIC ACID AT DIFFERENT TEMPERATURES

Escrivà-Cerdán^a, C., Blasco-Tamarit^a, E., García-García^a, D.M., García-Antón,
J.^{a,*}, Guenbour, A^b

^a*Ingeniería Electroquímica y Corrosión (IEC). Departamento de Ingeniería Química y Nuclear. ETSI Industriales. Universitat Politècnica de Valencia. PO Box 22012, E-46071 Valencia, Spain.*

*Tel. 34-96-387 76 39, Fax. 34-96-387 76 39, e-mail. jgarciaa@iqn.upv.es

^b*Laboratoire de Corrosion-Electrochimie, Faculté des Sciences, Université Mohammed V-Agdal, BP 1014 Rabat, Morocco.*

ABSTRACT

The influence of temperature and chloride concentration on the electrochemical behaviour of Alloy 31, a highly-alloyed austenitic stainless steel (UNS N08031) was studied in 40 wt.% polluted phosphoric acid solution. Polarization curves showed a stable passivation range at all the conditions studied. The results revealed that the material passivated spontaneously.

Passivation behaviour of Alloy 31 was investigated by using potentiostatic tests at different potentials. From the linear regions of the $\log i$ vs $\log t$ transients, the parameter n was obtained. The results showed that the applied potential hardly affects on the passivation rate n of Alloy 31.

Keywords: A. Stainless Steels, A. Acid Solutions, C. Passivity

1. INTRODUCTION

Phosphoric acid in pure state is not very corrosive compared to nitric or sulphuric acids. Ninety-five per cent of phosphoric acid is obtained by the wet process [1]. The main stages in this process involve the attack of phosphate ore by concentrated sulphuric acid (H_2SO_4 98%), filtration and concentration of acid. This technique generates severe corrosion problems due to the presence of impurities such as chlorides, fluorides and sulphides [1-4]. However, depending on the nature of phosphates and the type of phosphoric acid manufacturing process used, the equipment (reactors, agitators, pumps, drain, etc.) are subjected to slower or faster deterioration [1].

The choice of materials used in this industrial process plays an important role since they must have both good chemical and mechanical resistance. These two characteristics are not always easy to obtain and a trade-off between these properties must be reached [5]. In this sense, austenitic stainless steels are a good choice for phosphoric media. In this study, a highly alloyed austenitic stainless steel (UNS N08031) was used.

The major disadvantage of these alloys is their high cost compared with conventional stainless steels, due to the higher percentage of the alloying elements such as Cr, Ni and Mo, as well as the complexity of the manufacturing process [6].

The favourable effect of the alloying elements on the corrosion resistance is attributed to the formation of a protective passive surface film [7-9]. This film is stable, invisible, thin, durable and extremely adherent and self-repairing and its stability depends on the nature of the corroding metal and ion present in the solution [9]. In order to prevent

corrosion, it is of paramount importance that stainless steels have a stable passive film with rapid passivation even in severe corrosive environments [8]. It is believed that the stability of passive films and their passivation kinetics are subject to the influence of metallurgy, applied passivation potentials, pH and chloride ion concentration in aqueous solutions [8, 10-12]. Therefore, it is necessary to know the kinetics at which the passive film is formed on stainless steels.

The behaviour of stainless steels in aqueous acid solutions has been widely studied. In this sense, there are several references regarding to their corrosion behaviour in phosphoric acid [4, 5, 13, 14] and studies of the electrical properties of their passive films in this medium [15]. Other studies have reported the passivity and corrosion of austenitic stainless steels in sulphuric acid solutions [16-19], partly because of the extensive use of these alloys in acidic environments.

The aim of this study was to evaluate the corrosion behaviour of an austenitic stainless steel in phosphoric acid medium polluted with sulphate and chloride ions. The effects of chloride ion concentration and solution temperature on stainless steel corrosion behaviour and passivation kinetic behaviour were investigated.

2. EXPERIMENTAL PROCEDURE

2.1. MATERIALS AND SOLUTIONS

The material tested was the high-alloyed austenitic stainless steel UNS N08031 (Alloy 31) provided by Thyssen Krupp VDM. Material composition is shown in **Table 1**.

Alloy 31 electrodes were cylindrically shaped (8 mm in diameter and 55 mm long) and covered with a polytetrafluoroethylene (PTFE) coating. The area exposed to the solution was 0.5 cm². All specimens were abraded up to 4000 grit emery paper. Subsequently the electrode was rinsed with distilled water and was air-dried.

The potentiodynamic and potentiostatic experiments carried out in this work were performed in polluted 40 wt.% phosphoric acid (5.5 M) solution with 2 wt.% of H₂SO₄ (0.26 M) and two different concentrations of chlorides (prepared from KCl): 0.03 wt.% (380 ppm) and 0.2 wt.% (2528 ppm), typical for the phosphoric acid industry. According to the equilibrium diagram of phosphoric acid-sulphuric acid system, the pH-value of the solution is 0.42.

2.2. ELECTROCHEMICAL TESTS

Three different electrochemical tests were performed in this study. The tests were conducted in a horizontal three-electrode cell held at a constant temperature using a silver/silver chloride (Ag/AgCl) 3 M potassium chloride (KCl) electrode as a reference electrode (E vs. standard hydrogen electrode [SHE] = $E_{\text{Ag/AgCl [3M]}} + 0.206 \text{ V}$) and a platinum (Pt) wire as counter electrode. The experimental device consists of two elements [20, 21]: the electrochemical horizontal cell and the image acquisition unit formed by a trinocular microscope-stereoscope (NIKON SMZ-U) zoom 1:10 and a colour video camera (SONY SSC-C370P). This method allows the observation of the electrode surface in real-time, simultaneously to the electrochemical data acquisition without disturbing the electrochemical system [21]. In order to remove the oxygen

present in the system, the solution was deaerated by bubbling N₂ into the solution for 20 min before the test, and then the nitrogen atmosphere was maintained over the liquid surface during the whole test.

The experiments were conducted under thermostated conditions at 20, 40, 60 and 80 °C in order to study the influence of temperature on the corrosion behaviour of Alloy 31.

2.2.1. Open circuit potential measurements

The Open Circuit Potential was measured for 1 h in the test solutions. The average value of the potentials recorded during the last 300 s was the value of the OCP according to ASTM G-5 [22].

2.2.2. Potentiodynamic curves

Potentiodynamic polarisation curves of Alloy 31 were determined using a Solartron 1287 potentiostat. Before each polarisation measurement, the working electrodes were initially polarised in four steps from the OCP values to -400 mV_{Ag/AgCl}. This potential was maintained for 3600 s in order to remove the passive film formed previously and to create reproducible initial conditions. Then the sample was polarised anodically at a scan rate of 0.1667 mV/s from -400 mV_{Ag/AgCl} to the anodic direction.

From the ***E-log i*** plot, the corrosion potential (E_{corr}) and corrosion current density (i_{corr}) were obtained; in addition, the breakdown potential (E_b) was defined as the potential at which the current density reaches 100 $\mu\text{A}/\text{cm}^2$. The current density before E_b is almost

constant during a wide range of potentials and is defined as the passive current density (i_p). The tests were repeated at least three times.

2.2.3. Potentiostatic tests

Potentiostatic passivation tests were performed using an Autolab PGSTAT302N potentiostat in order to obtain the current transient at a constant applied potential. The potentiodynamic curves were used to set the four values of the imposed potentials (300, 500, 800 and 1000 mV_{Ag/AgCl}). Prior to each measurement, the working electrodes were polarised to -400 mV_{Ag/AgCl} for 3600 s to remove the passive film formed in air [23-25]. Then the chosen potential was applied for 1 h and the potentiostatic current density transients were recorded. It is noteworthy that the data acquisition was 250 points/s in order to record the highest number of points.

3. RESULTS AND DISCUSSION

3.1. OPEN CIRCUIT POTENTIALS

Figure 1 presents an example of the Open Circuit Potential (OCP) register for Alloy 31 in polluted 40 wt.% phosphoric acid with 2 wt.% H₂SO₄ and 0.03 wt.% of chloride ions at 20, 40, 60 y 80 °C. At all temperatures the potential shifted towards more positive values immediately after the immersion.

Alloy 31 registered an increase in OCP with time in both solutions studied, at any temperature. Moreover, no change was observed on its surface during the hour of immersion. Both facts indicated that the material was passivated.

The ennoblement of the potential observed in **Figure 1** is attributable to healing of the pre-immersion air-formed oxide film and further thickening of the oxide film as a result of the interaction between the electrolyte and the metal surface [26]. The growth of the oxide film continues until the film acquires a thickness that is stable in the electrolyte. Alloy 31 contains 26.75% chromium, which is a passivable element. Thus, during the OCP test the passive film containing Cr_2O_3 grew on the electrode surface, shifting the OCP value to higher potentials [27].

Table 2 summarises the OCP values for Alloy 31 in 40 wt.% H_3PO_4 solutions and 2 wt.% H_2SO_4 with chloride ion concentrations of 0.03 wt.% and 0.2 wt.% All the values are between $73 \text{ mV}_{\text{Ag}/\text{AgCl}}$ and $239 \text{ mV}_{\text{Ag}/\text{AgCl}}$, which correspond to the passive region of the alloy in these solutions as it will be commented below (*Section 3.2. Potentiodynamic curves*). As chloride concentration increases the OCP values shift to more active potentials at any temperature.

The displacement of the OCP values towards more positive values with increasing temperature in the tests conducted in the H_3PO_4 solutions (**Table 2**) is justified by the passive nature of Alloy 31. It is well known that temperature favours the kinetics of corrosion reactions [28-32], however it also promotes the fast growth of passive films on metallic surfaces [33-35], which causes the ennoblement of the metal.

The increase of chloride concentration in the solution causes a slight decrease in the OCP values (**Table 2**). According to Cardoso et al. [36] the presence of chloride leads to a decrease in this parameter, probably due to the partial dissolution of the passive film formed on the surface. Moreover, the harmful effect of temperature is greater in the solutions containing a higher concentration of chloride because this anion should make the oxide dissolve more easily.

3.2. POTENTIODYNAMIC CURVES

Potentiodynamic curves of Alloy 31 in polluted 40 wt.% H_3PO_4 with 2 wt.% H_2SO_4 and chloride ion concentrations of 0.03 wt.% (**Figure 2a**) and 0.2 wt.% (**Figure 2b**) were obtained at 20, 40, 60 and 80 °C to evaluate the effect of temperature and chloride concentration on the general corrosion resistance of the metal.

Polarisation curves of Alloy 31 in polluted 40 wt.% H_3PO_4 are characterised by a very wide potential domain of passivity at all the studied conditions ($\approx 1200 \text{ mV}_{\text{Ag}/\text{AgCl}}$ at 20 °C and 40 °C and $\approx 900 \text{ mV}_{\text{Ag}/\text{AgCl}}$ at 60 °C and 80 °C). The OCP values (**Table 2**) were in the passive zone of the potentiodynamic curves, which confirms the fact that Alloy 31 was spontaneously passivated.

In general, Alloy 31 registered a stable current density value during the passivation range in both solutions. Moreover, during the anodic scan the passive current density was very small, indicating the good corrosion resistance of Alloy 31 in the passive potential domain.

Temperature affects the cathodic reaction as it can be observed on the potentiodynamic curves (**Figure 2a** and **Figure 2b**), since the cathodic current densities increased with temperature in both polluted H_3PO_4 solutions. This shows that temperature favours the cathodic reaction [28, 37] and more specifically, it favours the Hydrogen Evolution Reaction (HER) which leads to an increase of H_2 generation. Temperature also favours the kinetics of the corrosion reactions, and especially the anodic dissolution of the metal, since the anodic current densities were higher as temperature increased. The abrupt increase of current density occurs at lower potentials as temperature increases, indicating that the loss of passivity of Alloy 31 occurs earlier as temperature increases from 20 to 80 °C in both polluted H_3PO_4 solutions.

It is noteworthy that at 60 and 80 °C the curves revealed the presence of three corrosion potentials, at which the anodic current density is equal to the cathodic current density, in the active, active-passive and passive region. Similar corrosion behaviour has been reported for chromium and chromium containing stainless steels in acid medium [38] and in acidic chloride solutions [24, 25, 39-41]. This behaviour is an indication of an unstable passive system. At low potentials the HER is dominant and gives a cathodic current density. At the first corrosion potential E_{corr1} , the cathodic current density equals the anodic current density and gives a stable corrosion potential. At a potential range between E_{corr1} and E_{corr2} the anodic current density is larger than the cathodic current density and presents net current density as anodic current density. After the passage of the active-passive transition (above E_{corr2}) the current density drops and again becomes cathodic. This behaviour has been attributed to the HER occurring on the passive surface at a rate greater than the rate of passive dissolution [40]. However, as it has been reported, the generation of metal cations that may affect cathodic depolarisation may

contribute to the observed effects on the corrosion potentials. This cathodic loop ends at a third corrosion potential after which the net current is again the anodic current. [24]

Therefore, the polarisation curves show three corrosion potentials when temperature increases above 40 °C. This phenomenon can be justified by the ideal polarisation curves in **Figure 3**. Curves A_1 and A_2 would represent the ideal anodic polarisation curves of Alloy 31 in the tested solutions and curves B_1 and B_2 represent the ideal cathodic reaction of H^+ reduction. In the case that the corrosion process was composed of cathodic curve B_1 and anodic curve A_1 , the system would only presents one corrosion potential. This situation corresponds to the experimental results obtained at 20 and 40 °C in both solutions. However, an increase in temperature shifts the anodic and cathodic curves to higher current density values. Thus, the anodic and cathodic curves are represented by A_2 and B_2 respectively, in which three points of intersection are revealed corresponding to E_{corr1} , E_{corr2} , E_{corr3} [24]. This explains the number of corrosion potentials at the temperatures of 60 and 80 °C observed in **Figure 2** for both solutions.

The Alloy 31 surface was observed during the potentiodynamic curves in order to study the corrosion attack on its surface. An example is shown in **Figure 4**. This figure shows images of Alloy 31 in the 40 wt.% H_3PO_4 solution polluted with 2 wt.% H_2SO_4 and 0.2 wt.% of chloride ions at 80 °C at different potentials. Image a shows the electrode surface at the initial potential of the potentiodynamic sweep. Image b shows the surface electrode in the passive region, after the corrosion potential. Image c corresponds to the potential of 800 mV_{Ag/AgCl}, before the breakdown potential (1028 mV_{Ag/AgCl}). In all these images, practically no damage is observed on the surface electrode. However, at higher potentials than the breakdown potential (image d and its magnified image f) it is

observed that the surface presents a light, uniform corrosion by comparison with image e, which corresponds to the magnified area of image a. Therefore, this fact suggests that the passive film has been broken.

In spite of the fact that the presence of chloride suggests pitting corrosion [32, 42, 43], the images of the surface electrode (**Figure 4**) revealed uniform corrosion on the electrode surface. **Figure 4f** shows in detail the aspect of the electrode surface after the potentiodynamic polarisation tests in the highest chloride concentration solution at the extreme temperature (80 °C). This image reveals some defects which could be related to pitting corrosion. However, they may be related to the appearance of metaestable pittings during the polarisation process. The formation of these defects was more obvious as temperature and chloride concentration increase. Moreover, when temperature increases the austenitic grains of Alloy 31 become distinguishable, as it is shown in **Figure 4f**.

In general, pitting corrosion is hardly observed on Alloy 31 under the conditions studied, even under the most severe conditions (the highest concentration of chloride ions and at 80 °C). In this sense, it has been reported that chloride and high temperatures affect film stability, but the film does not break up [36]. The dissolution of passivant species, such as metallic chloride, is favoured by the increased temperature.

It is also well known that pitting corrosion is initiated by the presence of chloride ions. Nevertheless, the high pitting corrosion resistance of Alloy 31 in this medium may be attributable to the chemical composition of this alloy, which has high Cr, Ni and Mo content. Nickel is able to reduce the corrosion rate [4] and high molybdenum content in

stainless steels is known to increase the resistance to localized and pitting corrosion [44]. The role of Ni and Mo in stainless steels at anodic potentials in acid solutions is to stabilise the passive film and to eliminate the active surface sites [4].

On the other hand, the increase of chloride ion concentration has not been found to have any effect on the cathodic reaction, as the comparison of **Figure 2a** and **Figure 2b** shows. However, the anodic current density slightly increased in the presence of a higher chloride concentration. This displacement is justified by the fact that chloride ions accelerate the anodic process by altering passivity and activating the material dissolution rate [45-47].

3.2.1. Electrochemical parameters

From the potentiodynamic curves, corrosion potential and corrosion current density values were obtained for the different conditions studied (**Table 3**).

In general, **corrosion potentials**, E_{corr} shifted towards more positive values with temperature in both solutions. This increase in corrosion potential seems to be related to the increase in cathodic current densities with temperature [28]. This displacement of the corrosion potentials is in agreement with the results reported by other authors [28, 34, 36], who studied the effects of the solution temperature on different stainless steels.

On the other hand, the higher concentration of chloride ions scarcely decreased the corrosion potentials, as observed from the E_{corr} data of the solution with higher Cl^- concentration, which are lower than those obtained in the solution with 0.03 %wt. of Cl^-

. In this sense, Iken et al. [4] showed that the presence of impurities increased the anodic process. This effect was attributed to adsorption of aggressive ions on the material surface, which prevented passivity [46] and accelerated local anodic dissolution.

Corrosion current densities, i_{corr} did not present any clear trend with temperature. The highest value of the corrosion current density was obtained at 40 °C in the polluted H_3PO_4 solution with 0.03 wt.% of chloride (**Table 3**), while in the solution with 0.2 wt.% of chloride the highest value was obtained at 20 °C. This seems to be related to the influence of the chlorides on the anodic reaction. Moreover, the results in **Table 3** reveal that, at temperatures of 60 and 80 °C, the values of i_{corr} are higher as the chloride concentration increased.

The **passivation current density, i_p** is observed to increase as temperature and chloride concentration increase (**Figure 5**). In general, the passive current densities are very low, indicating good passivation behaviour of the material. The increase of temperature favours the growth of the passive film, since temperature favours the kinetic reaction [28]. Alloy 31 contains 26.75% chromium, which is the main passive component of the passive film in the anodic polarisation of stainless steels [4]. Most authors agree that the film presents an inner layer of Cr_2O_3 and an outer layer of $Cr(OH)_3$ [36, 48, 49]. Wang [50] observed that phosphate was incorporated into the outer part of the passive film during the passivation process. Moreover, other researchers showed that phosphoric acid media favour the formation of iron phosphates [51]. In contact with the metallic substrates, phosphate species can produce an insoluble phosphate layer, which has a strong passivation characteristic [52]. The building up model of the phosphate layer and

the passivation of the metal was also proposed by Bouchemel [53] for titanium-copper alloys in phosphate solutions.

The **breakdown potential**, E_b of Alloy 31 decreases slightly as temperature increases (**Figure 6**) in both polluted H_3PO_4 solutions due to the fact that the anodic dissolution of the metal is favoured and this leads to a loss of passivity. This decrease is more pronounced in the solution with the highest chloride concentration. The effect of increasing the chloride concentration leads to a decrease in the breakdown potential, which suggested the ionic migration of the aggressive ions inside the passive film [45, 47].

The results show that the properties of the passive film formed under potential imposition slightly degraded with temperature. This fact was reflected by the lower breakdown potential, the higher passivation current densities and the narrower passivation ranges registered as the solution temperatures increased.

3.3. POTENTIOSTATIC MEASUREMENTS

Four potentials were selected on the passivity range of the polarisation curves of Alloy 31 in **Figure 2**. These potentials were 300, 500, 800 and 1000 $mV_{Ag/AgCl}$.

The current density-time curves of Alloy 31 were obtained at the four applied potentials (300, 500, 800 and 1000 $mV_{Ag/AgCl}$) in 40 wt.% H_3PO_4 polluted solutions with 0.03 wt.% and 0.2 wt.% of chloride. The values of current density corresponds to the total

current density resulting from the film formation and the dissolution of Alloy 31 in the solution [54].

The time trend of the potentiostatic current density can be expressed by the following empirical equation [25, 54, 55]:

$$i = A \cdot t^{-n} \quad (4)$$

where i denotes the anodic current density consumed in the building of the passive film, A is a constant, t is the time, and n is the passivation index, which is a constant value for a given environment-metal system. This parameter can be obtained from the linear region slope of the $\log i$ vs. $\log t$ plot:

$$\log i = \log A - n \cdot \log t \quad (5)$$

This parameter can be considered as an indirect measure of the rate of formation of the passive film upon the fresh metal surface, and depends on the applied anodic potential, among others [8, 25, 55, 56]. According to the literature [57, 58] $n = 1$ indicates the formation of a compact, highly protective passive film, while $n = 0.5$ indicates the presence of a porous film growing as a result of a dissolution and precipitation process.

Figure 7 and **figure 8** present the $\log i$ - $\log t$ plots for Alloy 31 in 40 wt.% H_3PO_4 solutions polluted with 2 wt.% H_2SO_4 , 0.03 wt.% and 0.2 wt.% of chloride respectively obtained at the selected passivation potentials. In these figures, the anodic current transients can be divided into three stages, as other authors did for austenitic stainless

steels [55, 59] and for aluminium and its alloys [56, 60]. The anodic current of the first stage was constant, indicating that the rate of oxide formation equalled the rate of oxide dissolution so that the oxide film hardly grew. The second stage belongs to a transition period in which the current density (i) starts to decrease. In the third stage, the anodic current density linearly decreased with time in the logarithmic scale. The current density drop was due to the fact that the formation rate of the passivating oxide film dominated over its dissolution rate on the bare surface [55, 56, 59, 60].

The current density-time transients presented in **Figure 7** and **Figure 8** show fluctuations at the end of the register. However, these fluctuations are more clearly observed as temperature increases and at the highest potentials, which may be due to the formation and further passivation of metaestable pitting [59, 61, 62].

In this study it has been found that the parameter n changes throughout the recorded time. In the second stage, and taking small intervals of time, the passivation rate was close to 0.5 indicating a porous film formation which grows by the dissolution and precipitation process. This value is related to the presence of phosphates in the solution [54]. However, in the linear region of the third stage, this parameter increases and generally comes close to 1, which means the formation of a high protective passive film on the stainless steel surface.

The variation of n with the applied potentials under the working conditions is summarised in **Table 4**. For the solution polluted with 0.03 wt.% of chloride, it can be clearly observed that n varies with temperature, decreasing as the temperature of the solution increases. However, when the solution containing 0.2 wt.% of chloride was

used, this tendency was not clearly observed, since the passivation rate n remains almost constant with temperature, although only slightly lower values of n were observed at 80 °C.

The parameter n was found to be higher in the solution with 0.2 wt.% of chloride than in the solution with 0.03 wt.% at a given applied potential. In general, n values of the highest concentrated solution were close to 1, which means that the growth rate of the passive film is higher than its destruction rate, and indicates the formation of a solid and compact film on the Alloy 31 surface [8, 56]. This phenomenon suggests the passivation effect of chloride ions in this acid solution. In fact, there is a competitive effect of chloride and phosphate ions in 40 wt.% H₃PO₄ solution [63] which hinders phosphates from being incorporated into the passive film, as a result the surface film become more compact [54].

On the other hand, these results show that the applied potential scarcely affects the passivation rate of Alloy 31 under the conditions studied. Thus, at a given temperature the value of n is almost constant, although it is noteworthy that in all cases n was slightly lower when the applied potential was 1000 mV_{Ag/AgCl}. This fact indicates that at the highest passivation potential, the passive film grew more slowly, probably due to the proximity of the breakdown potential, E_b .

4. CONCLUSIONS

OCP values obtained during the test indicate that Alloy 31 was spontaneously passivated under the studied conditions.

The potentiodynamic polarisation curves were characterised by a very wide range of passivity values indicating good protection efficiency.

The passive current density increased and the breakdown potential decreased as temperature increased in both solutions studied, involving a decrease in corrosion resistance with temperature.

The increase of the chloride concentration provokes a slight increase in the passive current densities and a decrease in the breakdown potential.

The study of the passivation behaviour has demonstrated that in general the passivation index n decreased as the solution temperature increases. The applied potentials were not found to have any effect on the parameter n , however it has shown a different trend at $1000 \text{ mV}_{\text{Ag/AgCl}}$ due to the proximity of the breakdown potential.

These results have revealed a formation of a passive film on Alloy 31 which protects it from corrosion attack. This passive film was found to be porous but later it became compact and highly protective.

Alloy 31 presents high corrosion resistance in solutions with chloride and sulphate ions in concentrations which simulate typical industrial conditions.

5. ACKNOWLEDGEMENTS

We wish to express our gratitude to the MAEC of Spain (PCI Mediterráneo C/8196/07, C/018046/08, D/023608/09 and D/030177/10), to Programa de Apoyo a la Investigación y Desarrollo de la UPV (PAID-06-09) and to the Generalitat Valenciana (GV/2011/093) for the financial support and to Asunción Jaime for her translation assistance.

6. REFERENCES

- [1] Pierre Becker, Phosphates and phosphoric acid: Raw materials, technology, and economics of the wet process, second ed., M. Dekker, New York, 1989.
- [2] A. Bellaouchou, A. Guenbour, A. Benbachir, Corrosion behavior of stainless-steel in phosphoric-acid polluted by sulfide ions, *Corrosion* 49 (1993) 656-662.
- [3] S. El Hajjaji, L. Aries, J. Audouard, F. Dabosi, The influence of alloying elements on the corrosion resistance of stainless steels in phosphoric acid medium polluted by sulphide ions, *Corros. Sci.* 37 (1995) 927-939.
- [4] H. Iken, R. Basseguy, A. Guenbour, A. B. Bachir, Classic and local analysis of corrosion behaviour of graphite and stainless steels in polluted phosphoric acid, *Electrochim. Acta* 52 (2007) 2580-2587.
- [5] A. Guenbour, M. A. Hajji, E. M. Jallouli, A. B. Bachir, Study of corrosion-erosion behaviour of stainless alloys in industrial phosphoric acid medium, *Appl. Surf. Sci.* 253 (2006) 2362-2366.

- [6] H. A. El Dahan, Pitting corrosion inhibition of 316 stainless steel in phosphoric acid chloride solutions. Part I: Potentiodynamic and potentiostatic polarization studies, *J. Mater. Sci.* 34 (1999) 851-857.
- [7] B. Jegdic, D. M. Drazic, J. P. Popic, Open circuit potentials of metallic chromium and austenitic 304 stainless steel in aqueous sulphuric acid solution and the influence of chloride ions on them, *Corros. Sci.* 50 (2008) 1235-1244.
- [8] J. B. Lee, Effects of alloying elements, Cr, Mo and N on repassivation characteristics of stainless steels using the abrading electrode technique, *Mater. Chem. Phys.* 99 (2006) 224-234.
- [9] A. M. M. Ibrahim, S. S. Abd El Rehim, M. M. Hamza, Corrosion behavior of some austenitic stainless steels in chloride environments, *Mater. Chem. Phys.* 115 (2009) 80-85.
- [10] N. De Cristofaro, M. Piantini, N. Zacchetti, The influence of temperature on the passivation behaviour of a super duplex stainless steel in a boric-borate buffer solution, *Corros. Sci.* 39 (1997) 2181-2191.
- [11] S. El Hajjaji, L. Aries, N. Pebere, F. Dabosi, J. P. Audouard, A. Benbachir, Passive state behavior of special austenitic and ferritic stainless steels in phosphoric acid polluted by sulfide ions, *Corrosion* 52 (1996) 865-871.
- [12] R. C. Newman, The dissolution and passivation kinetics of stainless alloys containing molybdenum. Coulometric studies of Fe-Cr and Fe-Cr-Mo alloys, *Corros. Sci.* 25 (1985) 331-339.

- [13] A. Bellaouchou, A. Guenbour, A. Benbachir, Corrosion Behavior of Stainless Steel in Phosphoric Acid Polluted by Sulfide Ions, *Corrosion* 49 (1993) 656-662.
- [14] A. Bellaouchou, A. Guenbour, A. Benbachir, The corrosion of an austenetic stainless steel in phosphoric acid: Effect of sulphide ions and abrasive action, *Bull. Electrochem.* 16 (2000) 166-170.
- [15] A. Guenbour, N. Bui, J. Faucheu, Y. Segui, A. Ben Bachir, F. Dabosi, The electrical properties of passive films formed on stainless steels in phosphoric acids, *Corros. Sci.* 30 (1990) 189-199.
- [16] G. T. Burstein, B. T. Daymond, The remarkable passivity of austenitic stainless steel in sulphuric acid solution and the effect of repetitive temperature cycling, *Corros. Sci.* 51 (2009) 2249-2252.
- [17] B. Jegdic, D. M. Drazic, J. P. Popic, Corrosion potential of 304 stainless steel in sulfuric acid, *J. Serbian Chem. Soc.* 71 (2006) 543-551.
- [18] D. A. Jones, N. D. Greene, Electrochemical measurement of low corrosion rates, *Corrosion* 22 (1966) 198-204.
- [19] K. S. Raja, D. A. Jones, Effects of dissolved oxygen on passive behavior of stainless alloys, *Corros. Sci.* 48 (2006) 1623-1638.
- [20] J. García Antón, A. Igual-Muñoz, J. L. Guiñón, V. Pérez-Herranz, A new technique for online visualization of the electrode surface under electrochemical corrosion processes, P-200002525 (2000), Spain.

- [21] J. García Antón, A. Igual-Muñoz, J. L. Guiñón, V. Pérez-Herranz, Horizontal electrochemical cell for electro-optical analysis of electrochemical processes, P-200002526 (2000), Spain.
- [22] ASTM G-5. Test Method for Making Potentiostatic and Potentiodynamic Anodic Polarization Measurements. ASTM (2004).
- [23] N. Li, Y. Li, S. Wang, F. Wang, Electrochemical corrosion behavior of nanocrystallized bulk 304 stainless steel, *Electrochim. Acta* 52 (2006) 760-765.
- [24] Y. X. Qiao, Y. G. Zheng, P. C. Okafor, W. Ke, Electrochemical behaviour of high nitrogen bearing stainless steel in acidic chloride solution: Effects of oxygen, acid concentration and surface roughness, *Electrochim. Acta* 54 (2009) 2298-2304.
- [25] Y. X. Qiao, Y. G. Zheng, W. Ke, P. C. Okafor, Electrochemical behaviour of high nitrogen stainless steel in acidic solutions, *Corros. Sci.* 51 (2009) 979-986.
- [26] E. A. Abd El Meguid, A. A. Abd El Latif, Critical pitting temperature for Type 254 SMO stainless steel in chloride solutions, *Corros. Sci.* 49 (2007) 263-275.
- [27] G. Lothongkum, S. Chaikittisilp, A. W. Lothongkum, XPS investigation of surface films on high Cr-Ni ferritic and austenitic stainless steels, *Appl. Surf. Sci.* 218 (2003) 203-210.
- [28] E. Blasco-Tamarit, A. Igual-Muñoz, J. García Antón, D. García-García, Effect of temperature on the corrosion resistance and pitting behaviour of Alloy 31 in LiBr solutions, *Corros. Sci.* 50 (2008) 1848-1857.

- [29] L. F. Garfias-Mesias, J. M. Sykes, Metastable pitting in 25 Cr duplex stainless steel, *Corros. Sci.* 41 (1999) 959-987.
- [30] A. Igual Munoz, J. García Antón, S. López Nuévalos, J. L. Guiñón, V. Pérez Herranz, Corrosion studies of austenitic and duplex stainless steels in aqueous lithium bromide solution at different temperatures, *Corros. Sci.* 46 (2004) 2955-2974.
- [31] N. J. Laycock, Effects of temperature and thiosulfate on chloride pitting of austenitic stainless steels, *Corrosion* 55 (1999) 590-595.
- [32] A. Pardo, E. Otero, M. C. Merino, M. D. Lopez, M. V. Utrilla, F. Moreno, Influence of pH and chloride concentration on the pitting and crevice corrosion behavior of high-alloy stainless steels, *Corrosion* 56 (2000) 411-418.
- [33] D. H. Hur, Y. S. Park, Effect of temperature on the pitting behavior and passive film characteristics of alloy 600 in chloride solution, *Corrosion* 62 (2006) 745-750.
- [34] A. Igual-Muñoz, J. García-Antón, J. L. Guiñón, V. Pérez-Herranz, Effects of solution temperature on localized corrosion of high nickel content stainless steels and nickel in chromated LiBr solution, *Corros. Sci.* 48 (2006) 3349-3374.
- [35] C. O. A. Olsson, D. Landolt, Passive films on stainless steels--chemistry, structure and growth, *Electrochim. Acta* 48 (2003) 1093-1104.
- [36] M. V. Cardoso, S. T. Amaral, E. M. A. Martini, Temperature effect in the corrosion resistance of Ni-Fe-Cr alloy in chloride medium, *Corros. Sci.* 50 (2008) 2429-2436.

- [37] M. Ibáñez-Ferrándiz, M. Blasco-Tamarit, D. M. García-García, J. García-Antón, A. Guenbour, S. Bakour, A. Benckokroun, Effect of temperature on the corrosion resistance of stainless steels in polluted phosphoric acid, *ECS Trans.* 25 (2010) 49-61.
- [38] E. E. Oguzie, J. Li, Y. Liu, D. Chen, Y. Li, K. Yang, F. Wang, The effect of Cu addition on the electrochemical corrosion and passivation behavior of stainless steels, *Electrochim. Acta* 55 (2010) 5028-5035.
- [39] B. E. Wilde, F. G. Hodge, The cathodic discharge of hydrogen on active and passive chromium surfaces in dilute sulphuric acid solutions, *Electrochim. Acta* 14 (1969) 619-627.
- [40] L. Bjornkvist, I. Olefjord, The electrochemistry of chromium in acidic chloride solutions: Anodic dissolution and passivation, *Corros. Sci.* 32 (1991) 231-242.
- [41] J. P. Popic, D. M. Drazic, Electrochemistry of active chromium: Part II. Three hydrogen evolution reactions on chromium in sulfuric acid, *Electrochim. Acta* 49 (2004) 4877-4891.
- [42] S. Zor, M. Soncu, L. Āapan, Corrosion behavior of G-X CrNiMoNb 18-10 austenitic stainless steel in acidic solutions, *J. Alloys Compd.* 480 (2009) 885-888.
- [43] A. Pardo, M. C. Merino, A. E. Coy, F. Viejo, R. Arrabal, E. Matykina, Pitting corrosion behaviour of austenitic stainless steels - combining effects of Mn and Mo additions, *Corros. Sci.* 50 (2008) 1796-1806.

- [44] L. Wegrelius, F. Falkenberg, I. Olefjord, Passivation of stainless steels in hydrochloric acid, *J. Electrochem. Soc.* 146 (1999) 1397-1406.
- [45] S. S. A. El Rehim, S. A. M. Refaey, F. Taha, M. B. Saleh, R. A. Ahmed, Corrosion inhibition of mild steel in acidic medium using 2-amino thiophenol and 2-cyanomethyl benzothiazole, *J. Appl. Electrochem.* 31 (2001) 429-435.
- [46] P. Marcus, The Role of Alloyed Elements and Adsorbed Impurities in Passivation of Metal-Surfaces, *J. Chim. Phys. Phys.- Chim. Biol.* 88 (1991) 1697-1711.
- [47] S. A. M. Refaey, Inhibition of chloride pitting corrosion of mild steel by sodium gluconate, *Appl. Surf. Sci.* 157 (2000) 199-206.
- [48] M. Drogowska, H. Menard, L. Brossard, Electrooxidation of stainless steel AISI 304 in carbonate aqueous solution at pH8, *J. Appl. Electrochem.* 26 (1996) 217-225.
- [49] M. Drogowska, L. Brossard, H. Menard, 304 stainless steel oxidation in sulfate and sulfate plus bicarbonate solutions, *J. Appl. Electrochem.* 28 (1998) 491-501.
- [50] H. Wang, J. A. Turner, Austenitic stainless steels in high temperature phosphoric acid, *J. Power Sources* 180 (2008) 803-807.
- [51] M. Reffass, R. Sabot, M. Jeannin, C. Berziou, P. Refait, Effects of phosphate species on localised corrosion of steel in $\text{NaHCO}_3+\text{NaCl}$ electrolytes, *Electrochim. Acta* 54 (2009) 4389-4396.

- [52] S. R. Moraes, D. Huerta-Vilca, A. J. Motheo, Corrosion protection of stainless steel by polyaniline electrosynthesized from phosphate buffer solutions, *Prog. Org. Coat.* 48 (2003) 28-33.
- [53] H. Bouchemel, A. Benchettara, Corrosion behaviour of Ti40Cu60 alloy in H₃PO₄ solutions, *Mater. Chem. Phys.* 115 (2009) 572-577.
- [54] M. Lakatos-Varsányi, F. Falkenberg, I. Olefjord, The influence of phosphate on repassivation of 304 stainless steel in neutral chloride solution, *Electrochim. Acta* 43 (1998) 187-197.
- [55] R. M. Fernández-Domene, E. Blasco-Tamarit, D. M. García-García, J. García-Antón, Repassivation of the damage generated by cavitation on UNS N08031 in a LiBr solution by means of electrochemical techniques and Confocal Laser Scanning Microscopy, *Corros. Sci.* 52 (2010) 3453-3464.
- [56] J. d. Kim, S. i. Pyun, Effects of electrolyte composition and applied potential on the repassivation kinetics of pure aluminium, *Electrochim. Acta* 40 (1995) 1863-1869.
- [57] J. R. Galvele, R. M. Torresi, R. M. Carranza, Passivity breakdown, its relation to pitting and stress-corrosion-cracking processes, *Corros. Sci.* 31 (1990) 563-571.
- [58] Z. Szklarska-Smialowska, Pitting corrosion of aluminum, *Corros. Sci.* 41 (1999) 1743-1767.
- [59] J. J. Park, S. I. Pyun, W. J. Lee, H. P. Kim, Effect of bicarbonate ion additives on pitting corrosion of type 316L stainless steel in aqueous 0.5 M sodium chloride solution, *Corrosion* 55 (1999) 380-387.

- [60] S. i. Pyun, E. J. Lee, Effect of halide ion and applied potential on repassivation behaviour of Al-1 wt.%Si-0.5 wt.%Cu alloy, *Electrochim. Acta* 40 (1995) 1963-1970.
- [61] G. T. Burstein, C. Liu, R. M. Souto, The effect of temperature on the nucleation of corrosion pits on titanium in Ringer's physiological solution, *Biomaterials* 26 (2005) 245-256.
- [62] G. O. Ilevbare, G. T. Burstein, The inhibition of pitting corrosion of stainless steels by chromate and molybdate ions, *Corros. Sci.* 45 (2003) 1545-1569.
- [63] B. Hammouti, K. Bekkouche, S. Kertit, Corrosion of steel in isoacidic 5.5 M H_3PO_4 solutions, *Bull. Electrochem.* 14 (1998) 49-51.

Figure captions

Figure 1. The variation of the open circuit potential with time for the Alloy 31 registered during 1 hour at 20, 40, 60 and 80 °C in 40 wt.% polluted phosphoric acid with 0.03 wt.% of chloride ions and 2 wt.% of H_2SO_4 .

Figure 2. Potentiodynamic curves of Alloy 31 in polluted 40 wt.% H_3PO_4 with 0.03 wt.% (a) and 0.2 wt.% (b) of chloride ions.

Figure 3. Supposed diagram of ideal polarization curves for Alloy 31 in polluted 40 wt.% H_3PO_4 at different temperatures.

Figure 4. Images (a-d) of Alloy 31 in 40 wt.% H_3PO_4 polluted with 2 wt.% H_2SO_4 and 0.2 wt.% of chloride ions at different potentials of the potentiodynamic test at 80 °C. Images e and f belong with the magnified section of images a and d, respectively.

Figure 5. Passivation current densities of Alloy 31 at different temperatures in the 40 wt.% H_3PO_4 solutions studied.

Figure 6. Breakdown potentials of Alloy 31 at different temperatures in the 40 wt.% H_3PO_4 solutions studied.

Figure 7. $\log i$ vs. $\log t$ transients for Alloy 31 in 40 wt.% H_3PO_4 polluted with 2 wt.% H_2SO_4 and 0.03 wt.% of chloride ions at (a) 20 °C, (b) 40 °C, (c) 60 °C and (d) 80 °C (potential values in $V_{\text{Ag}/\text{AgCl}}$).

Figure 8. $\log i$ vs. $\log t$ transients for Alloy 31 in 40 wt.% H_3PO_4 polluted with 2 wt.% H_2SO_4 and 0.2 wt.% of chloride ions at (a) 20 °C, (b) 40 °C, (c) 60 °C and (d) 80 °C (potential values in $V_{\text{Ag}/\text{AgCl}}$).

Table captions

Table 1. Chemical composition of the UNS N08031 (Alloy 31) (wt.%).

Table 2. OCP values of Alloy 31 in the 40 wt.% H_3PO_4 solutions polluted with 2 wt.% H_2SO_4 and different concentrations of chloride ions at different temperatures.

Table 3. Chloride and temperature influence on the corrosion potentials and corrosion current densities in polluted 40 wt.% H_3PO_4 with 2 wt.% H_2SO_4 and different concentrations of chloride ions.

Table 4. The slopes n of current decay transients in the $\log i$ - $\log t$ for passivation of Alloy 31 in 40 wt.% H_3PO_4 polluted with 2 wt.% H_2SO_4 and different concentrations of chloride ions.

Table 1

	%Cr	%Fe	%Ni	%Mo	%Mn	%Cu	%N	%Si	%C	%S	%P
Alloy 31	26.75	31.43	31.85	6.6	1.5	1.21	0.193	0.1	0.005	0.002	0.017

Table 2

Temperature (°C)	OCP ($\text{mV}_{\text{Ag/AgCl}}$)	
	0.03 wt.% Cl ⁻	0.2 wt.% Cl ⁻
20	133	73
40	168	116
60	198	148
80	239	186

Table 3

T (°C)	0.03 wt.% Cl ⁻		0.2 wt.% Cl ⁻	
	E _{corr} (mV _{Ag/AgCl})	i _{corr} (μA/cm ²)	E _{corr} (mV _{Ag/AgCl})	i _{corr} (μA/cm ²)
20	-154	0.50	-233	12.30
40	-183	4.60	-194	1.92
60	118	0.96	144	1.75
80	231	1.01	205	1.69

Table 4

E_{apl} ($V_{\text{Ag/AgCl}}$)	20 °C		40 °C		60 °C		80 °C	
	0.03 wt.% Cl ⁻	0.2 wt.% Cl ⁻						
0.3	0.961	0.942	0.858	0.992	0.670	0.967	0.536	0.745
0.5	0.974	0.961	0.878	0.993	0.731	0.926	0.606	0.710
0.8	0.979	0.971	0.868	1.008	0.751	0.993	0.596	0.662
1	0.920	0.859	0.734	0.786	0.671	0.521	0.526	0.491

Figure 1

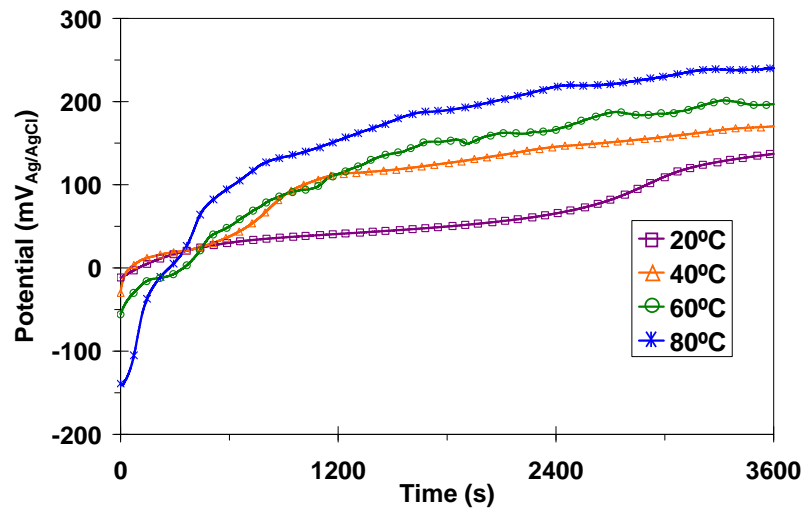


Figure 2

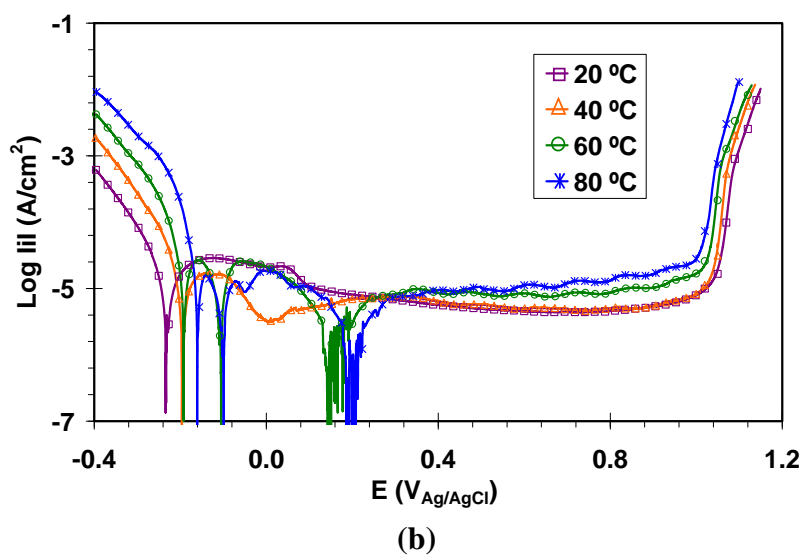
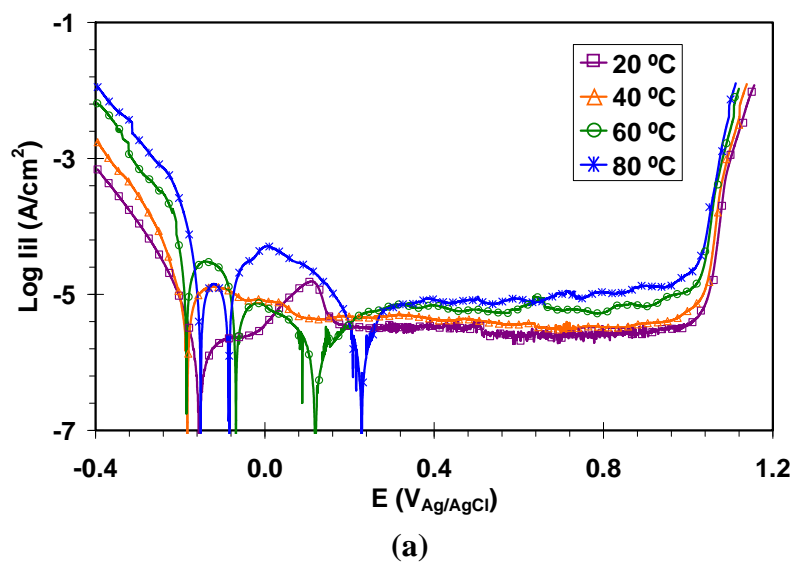


Figure 3

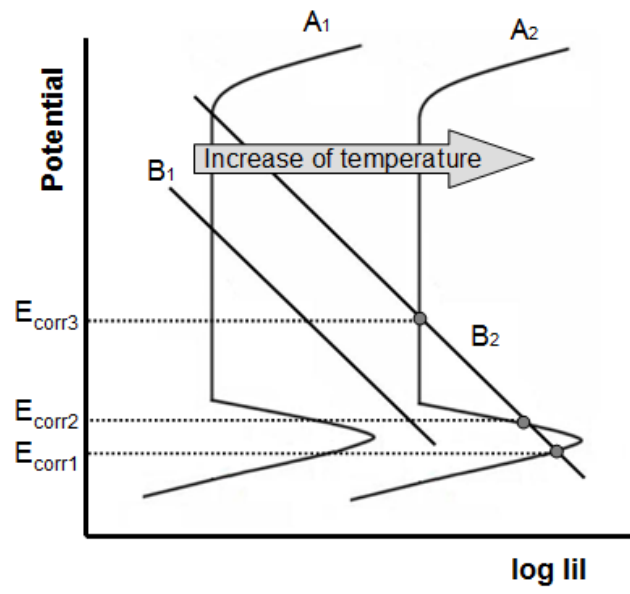
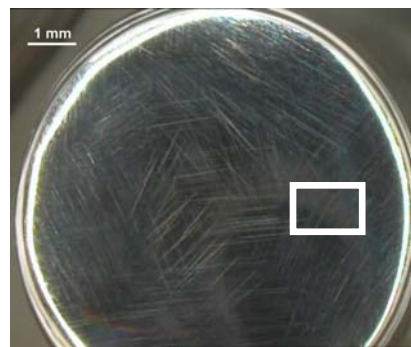
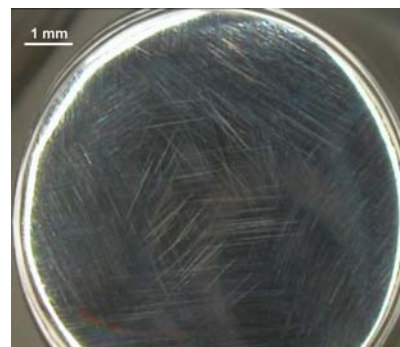


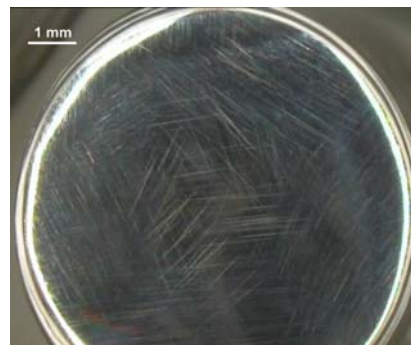
Figure 4



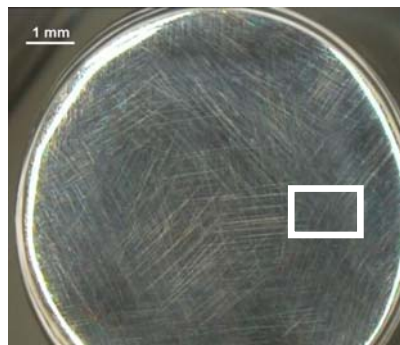
(a) $E = 50 \text{ mV}_{\text{Ag/AgCl}}$



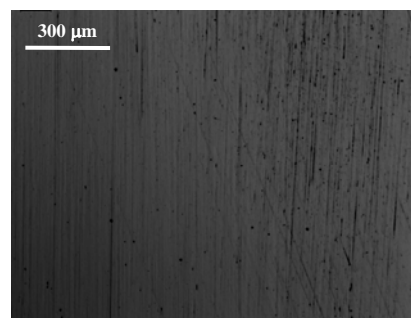
(b) $E = 300 \text{ mV}_{\text{Ag/AgCl}}$



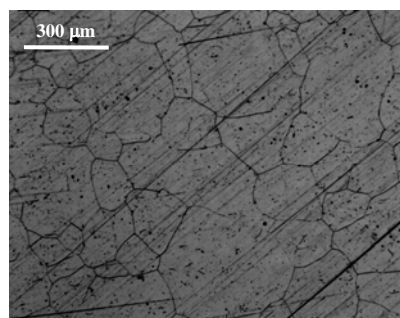
(c) $E = 800 \text{ mV}_{\text{Ag/AgCl}}$



(d) $E = 1060 \text{ mV}_{\text{Ag/AgCl}}$



(e) $E = 50 \text{ mV}_{\text{Ag/AgCl}}$



(f) $E = 1060 \text{ mV}_{\text{Ag/AgCl}}$

Figure 5

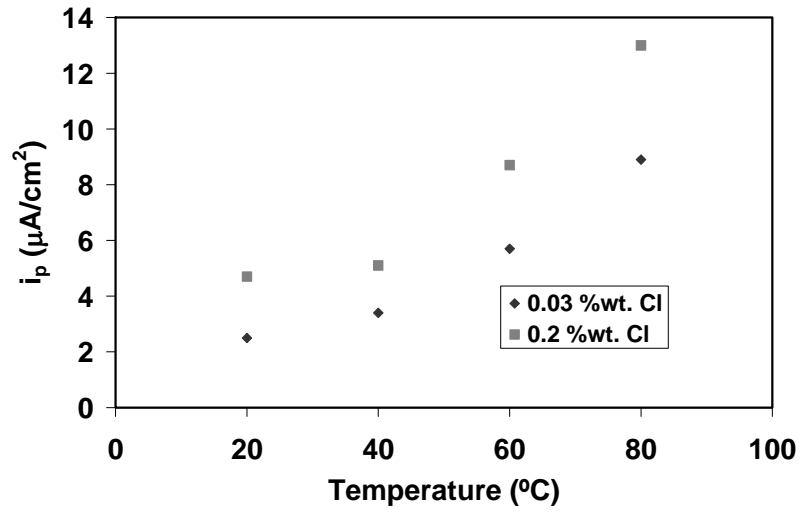


Figure 6

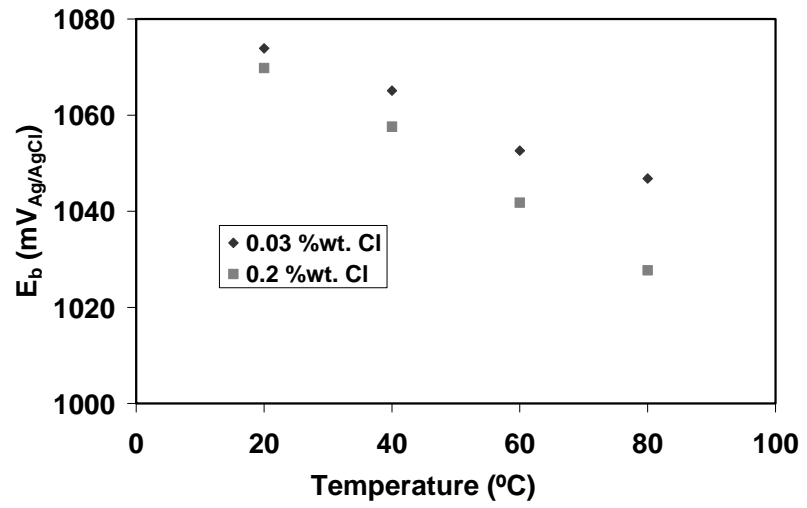
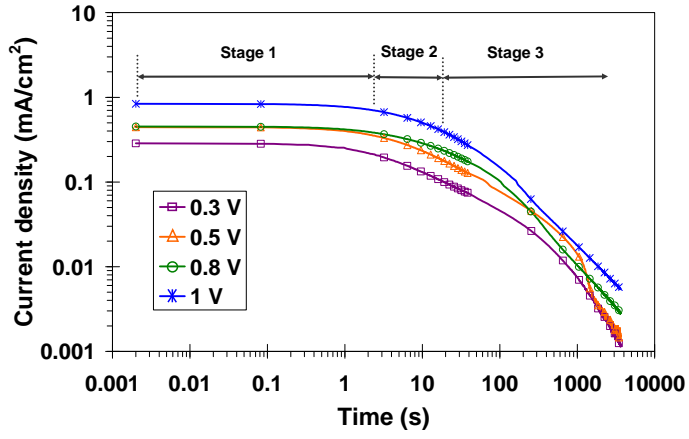
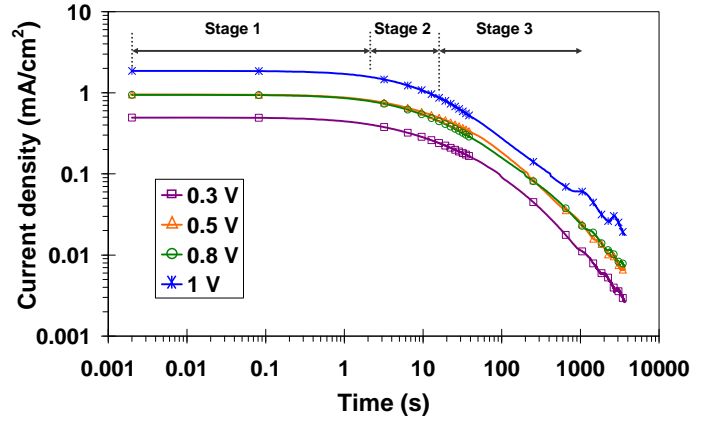


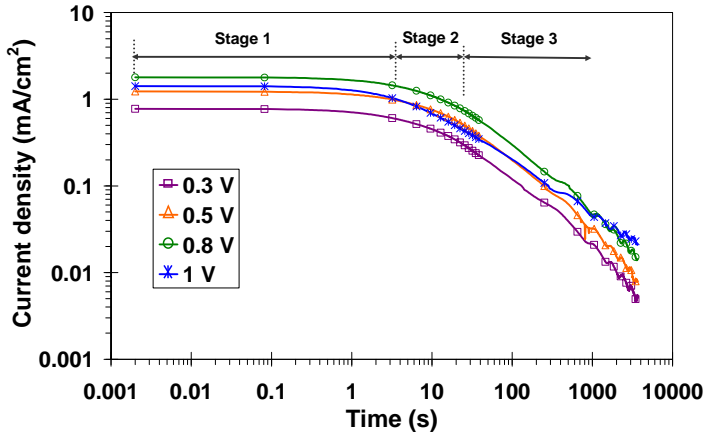
Figure 7



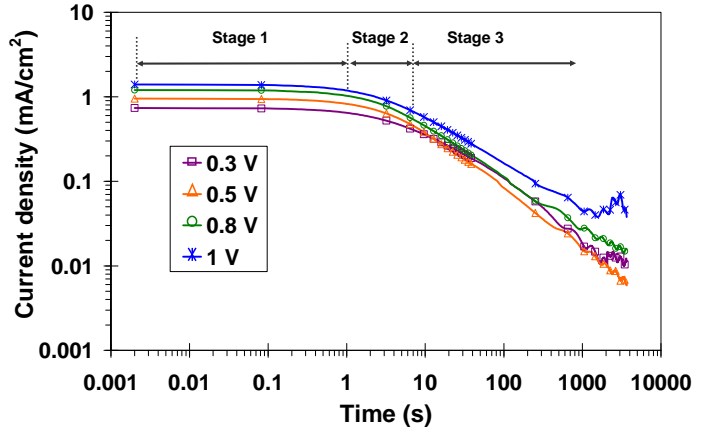
(a)



(b)

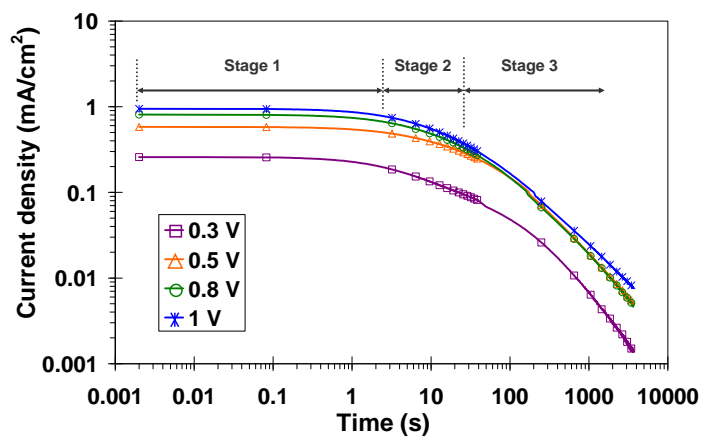


(c)

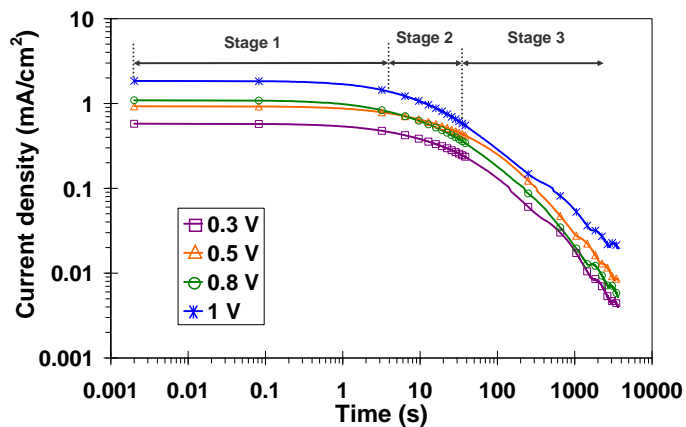


(d)

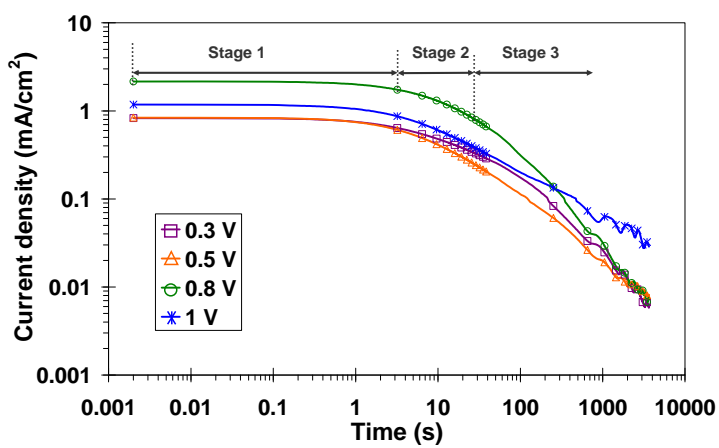
Figure 8



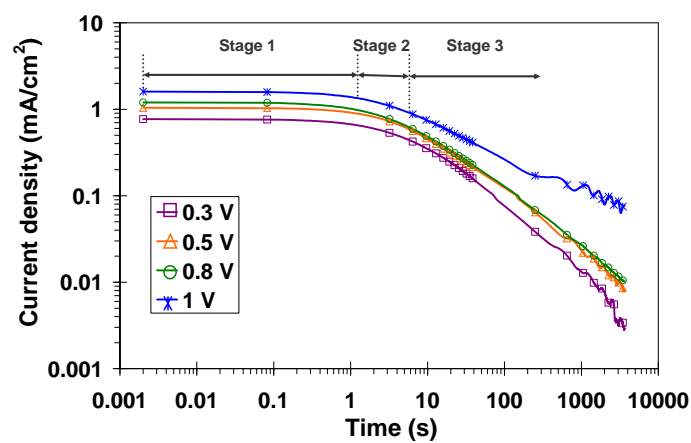
(a)



(b)



(c)



(d)